

PAC study of dynamic hyperfine interactions at ^{111}In -doped Sc_2O_3 semiconductor and comparison with *ab initio* calculations

E. L. Muñoz¹, D. Richard¹, A.W. Carbonari²,
L. A. Errico¹ and M. Rentería¹

¹Departamento de Física and IFLP (CONICET), La Plata, Argentina,

² Instituto de Pesquisas Energéticas y Nucleares, São Paulo, Brazil

Motivations

- The inclusion of impurities in semiconductors have broad significance for the basic and applied research.

Motivations

- The inclusion of impurities in semiconductors have broad significance for the basic and applied research.
- The experimental characterizations at impurity sites in oxides have a fundamental importance for the evaluation of the *ab initio electronic structure calculation* predictions of structural and electronic properties in doped systems.

Motivations

- The inclusion of impurities in semiconductors have broad significance for the basic and applied research.
- The experimental characterizations at impurity sites in oxides have a fundamental importance for the evaluation of the *ab initio electronic structure calculation* predictions of structural and electronic properties in doped systems.
- To correctly understand the underlying physics of the phenomenological model used in perturbation factors it is necessary a theoretical study based in first-principles calculations.

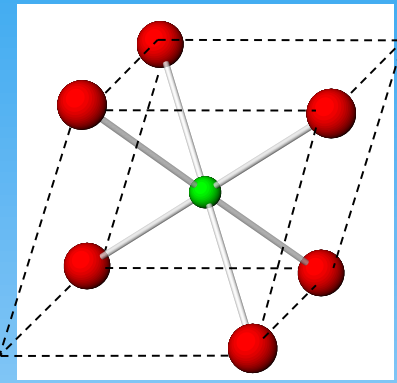
Outline

- Studied system
- PAC technique
- Experimental results
- FP-APW+lo calculations
- Final remarks

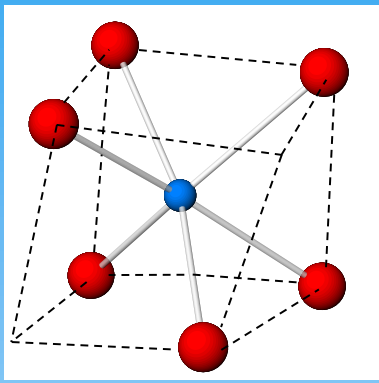
Outline

- Studied system
- PAC technique
- Experimental results
- FP-APW+lo calculations
- Final remarks

Studied system: Sc_2O_3



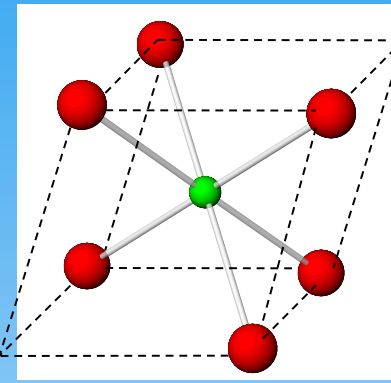
Site D



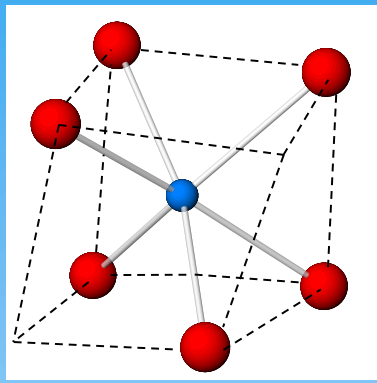
Site C

- The Sc_2O_3 oxide crystallizes in the bixbyite structure and presents two cation sites: C and D.
- The relative abundance is $f_C/f_D = 3:1$.
- The ONN coordination is 6 for both sites.
- The D site is axially symmetric and the C site presents high asymmetry.

Studied system: Sc_2O_3



Site D



Site C

- The Sc_2O_3 oxide crystallizes in the bixbyite structure and presents two cation sites: C and D.
- The relative abundance is $f_C/f_D = 3:1$.
- The ONN coordination is 6 for both sites.
- The D site is axially symmetric and the C site presents high asymmetry.

Method	a (\AA)	$-u$	x	y	z
Experimental [1]	9.845	0.03546	0.39137	0.15477	0.38137
FP-APW+lo (LDA)	9.708	0.0364	0.3915	0.1545	0.3810
FP-APW+lo (WC-GGA)	9.798	0.0361	0.3913	0.1543	0.3812

[1] M. Marezio, Acta Cryst. **20**, 723 (1966).

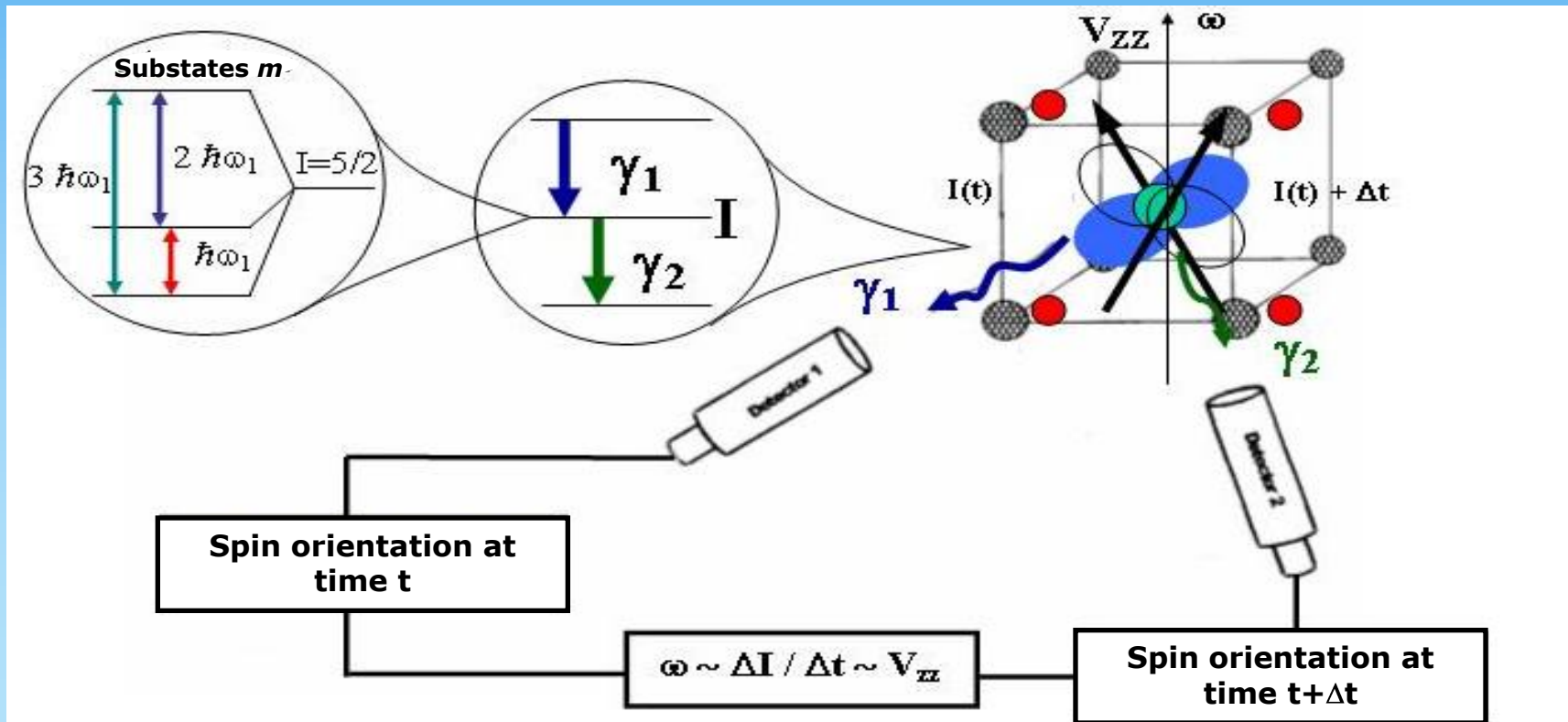
Outline

- Studied system
- PAC technique
- Experimental results
- FP-APW+lo calculations
- Final remarks

PAC technique

$$G_{22}^s(t) = S_{20}(\eta) + \sum_{n=1}^3 S_{2n}(\eta) \cos(\omega_n(\eta, \omega_Q)t)$$

$$R(t) = 2 \frac{C(180^\circ, t) - C(90^\circ, t)}{C(180^\circ, t) + 2C(90^\circ, t)}, \quad \omega_Q = \frac{eQV_{33}}{40\hbar}, \quad \eta = \frac{V_{11} - V_{22}}{V_{33}}$$

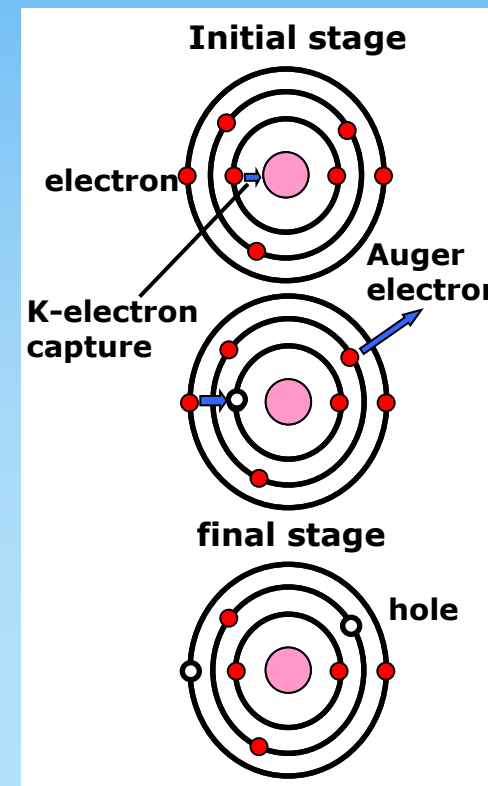
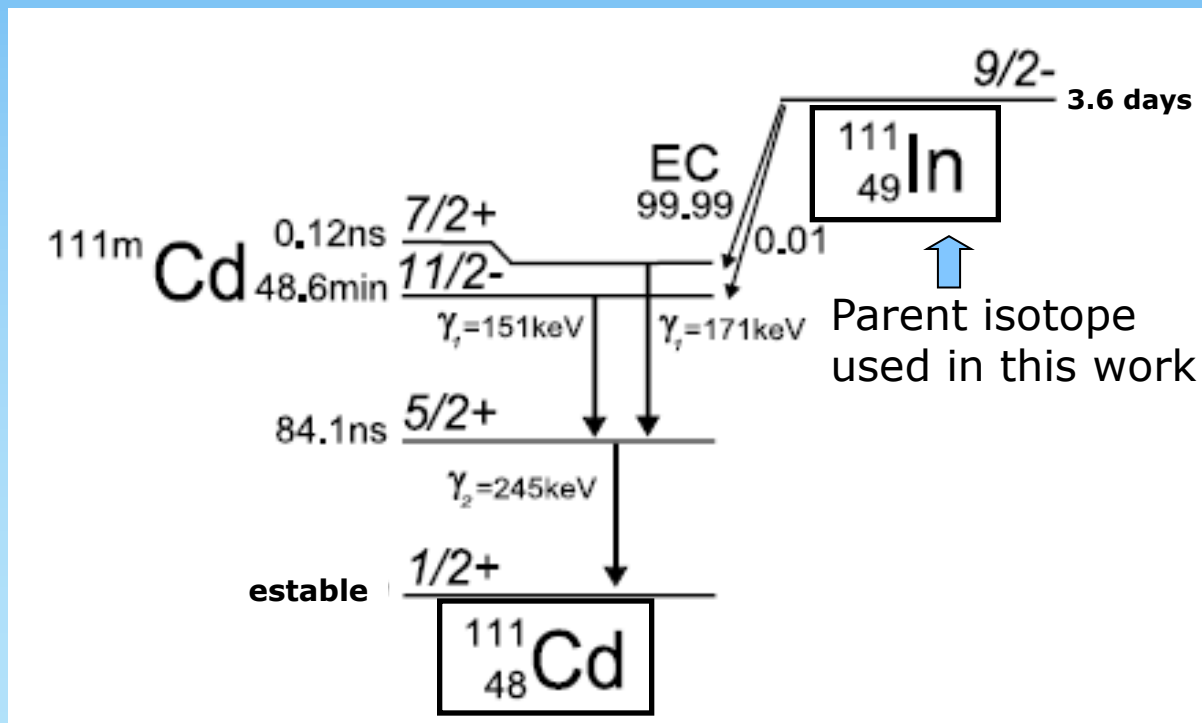


^{111}Cd probe and sample preparation

- Some drops of $^{111}\text{InCl}_3$ were deposited onto a Sc_2O_3 (99.999% purity) powder pellet. The ^{111}In thermal diffusion was performed in N_2 atmosphere (3×10^8 Pa) in steps from 423 K to 1073 K. The temperature dependence of the EFG was measured in the temperature range 10 K – 900 K.

^{111}Cd probe and sample preparation

➤ Some drops of $^{111}\text{InCl}_3$ were deposited onto a Sc_2O_3 (99.999% purity) powder pellet. The ^{111}In thermal diffusion was performed in N_2 atmosphere (3×10^8 Pa) in steps from 423 K to 1073 K. The temperature dependence of the EFG was measured in the temperature range 10 K – 900 K.



Dynamic Hyperfine Interactions: Bäverstam and Othaz model

$$G_{22}(t) = G_{22}^s(t) \cdot G_{22}^d(t)$$

λ_r : Abragam and Pound constant

λ_g : recovery constant ($\lambda_g^{-1} = \tau_g$)

$$\lambda_g = \gamma(1 - \alpha)$$

$$\lambda_r = \alpha\gamma$$

$$G_{22}^d(t) = \frac{\lambda_g}{\lambda_g + \lambda_r} + \frac{\lambda_r}{\lambda_g + \lambda_r} e^{-(\lambda_g + \lambda_r)t}$$

$$\left. \begin{aligned} \alpha &= \frac{\lambda_r}{\lambda_g + \lambda_r} \\ \gamma &= \lambda_g + \lambda_r \\ G_{22}^d(t) &= (1 - \alpha) + \alpha e^{-\gamma t} \end{aligned} \right\} \leftrightarrow \left. \begin{aligned} \lambda_g &= \gamma(1 - \alpha) \\ \lambda_r &= \alpha\gamma \end{aligned} \right\}$$

Dynamic Hyperfine Interactions: Bäverstam and Othaz model

$$G_{22}(t) = G_{22}^s(t) \cdot G_{22}^d(t)$$

λ_r : Abragam and Pound constant

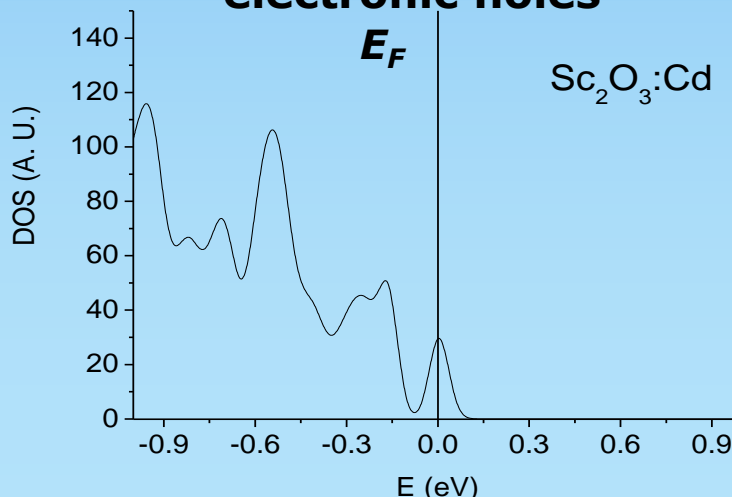
λ_g : recovery constant ($\lambda_g^{-1} = \tau_g$)

$$\lambda_g = \gamma(1 - \alpha)$$

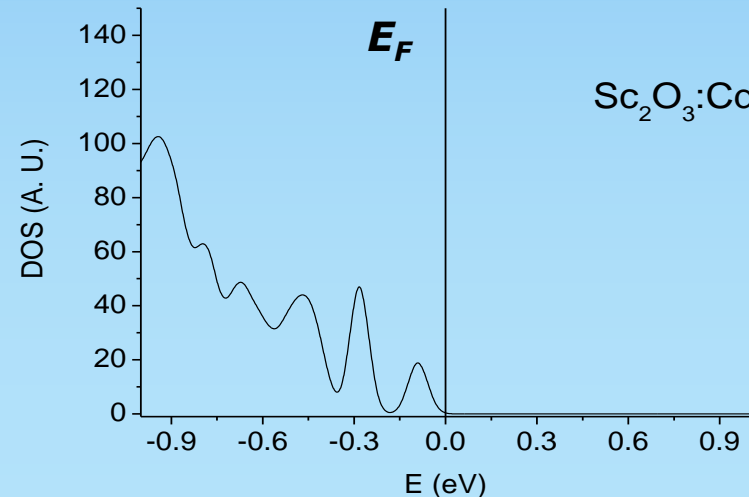
$$\lambda_r = \alpha\gamma$$

$$G_{22}^d(t) = \frac{\lambda_g}{\lambda_g + \lambda_r} + \frac{\lambda_r}{\lambda_g + \lambda_r} e^{-(\lambda_g + \lambda_r)t}$$

**State with
electronic holes**



**State without
electronic holes**



$$\alpha = \frac{\lambda_r}{\lambda_g + \lambda_r}$$

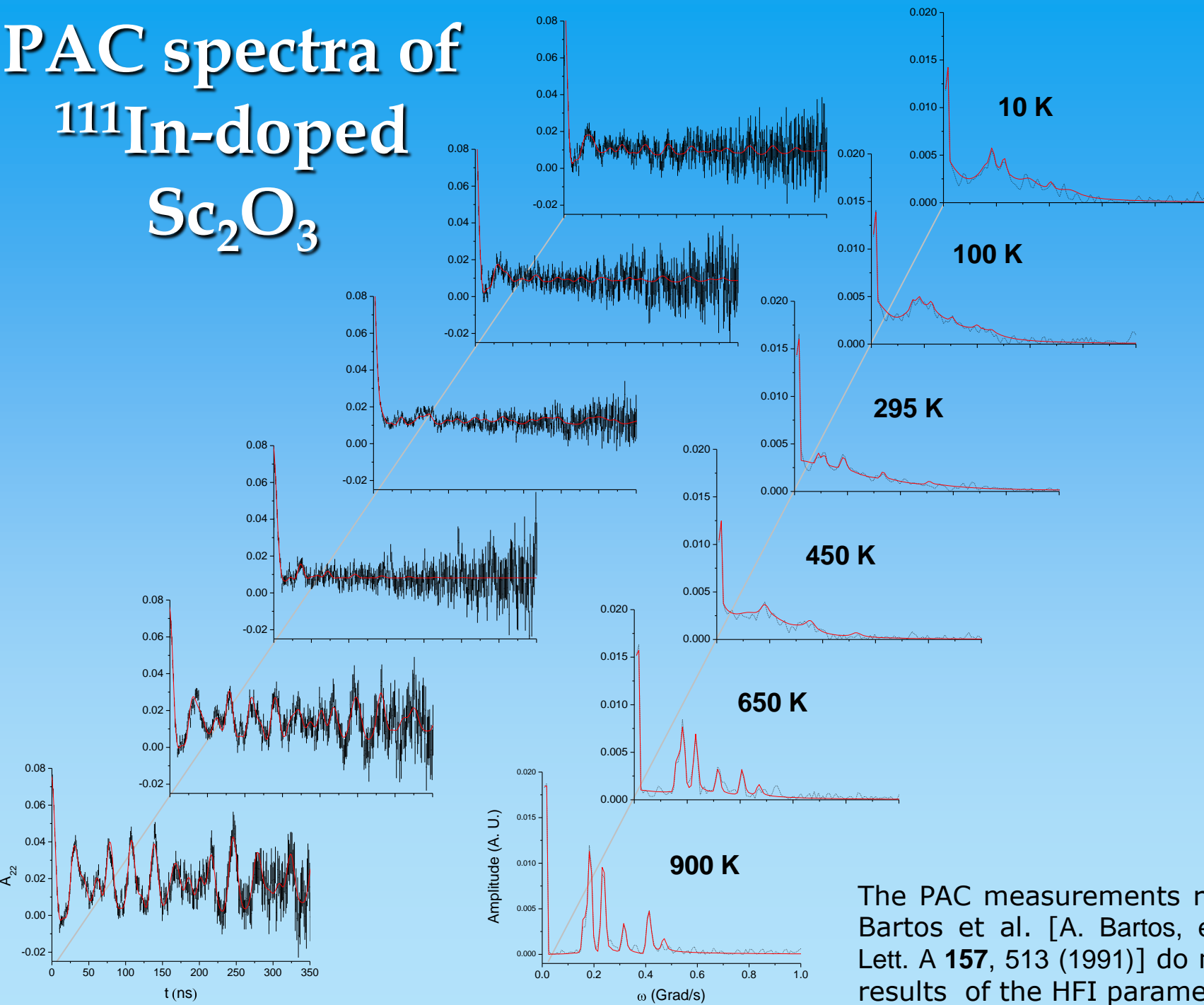
$$\gamma = \lambda_g + \lambda_r$$

$$G_{22}^d(t) = (1 - \alpha) + \alpha e^{-\gamma t}$$

Outline

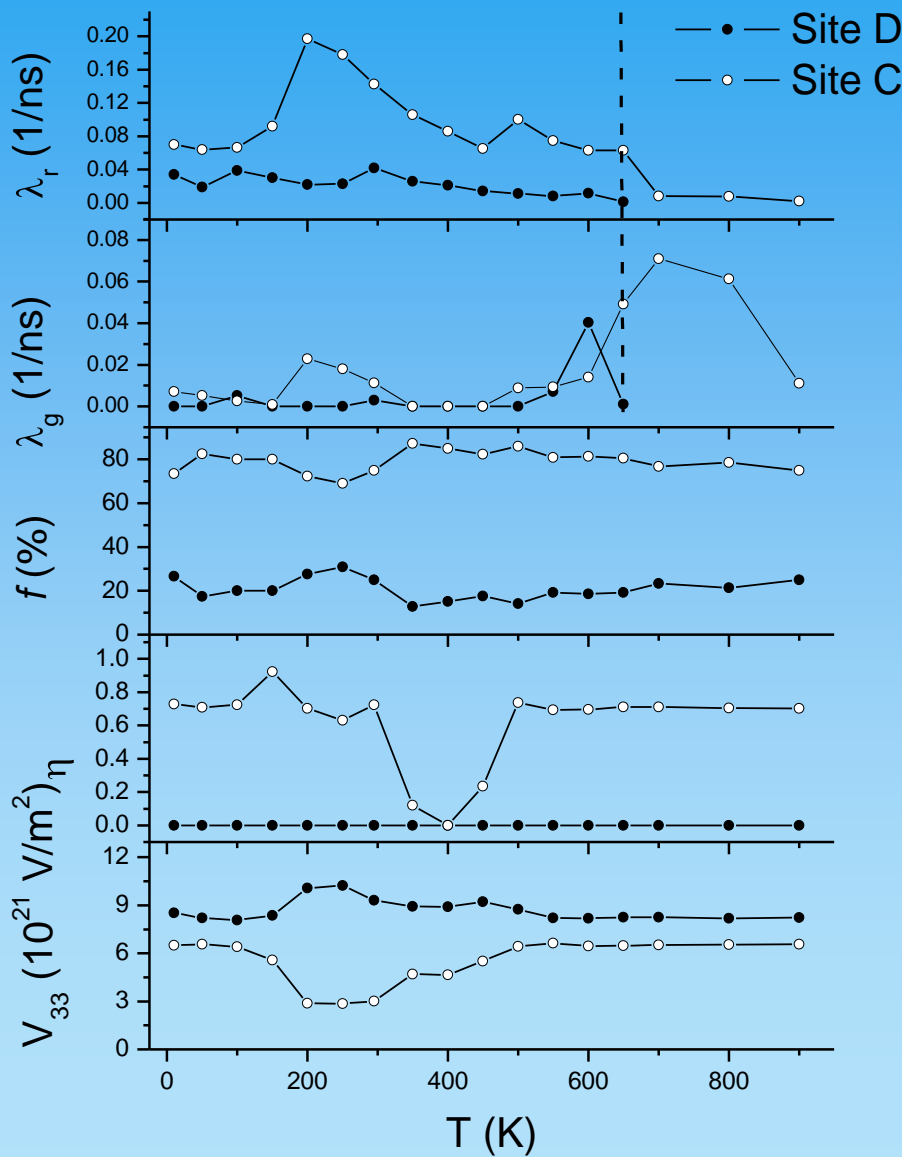
- Studied system
- PAC technique
- **Experimental results**
- FP-APW+lo calculations
- Final remarks

PAC spectra of ^{111}In -doped Sc_2O_3

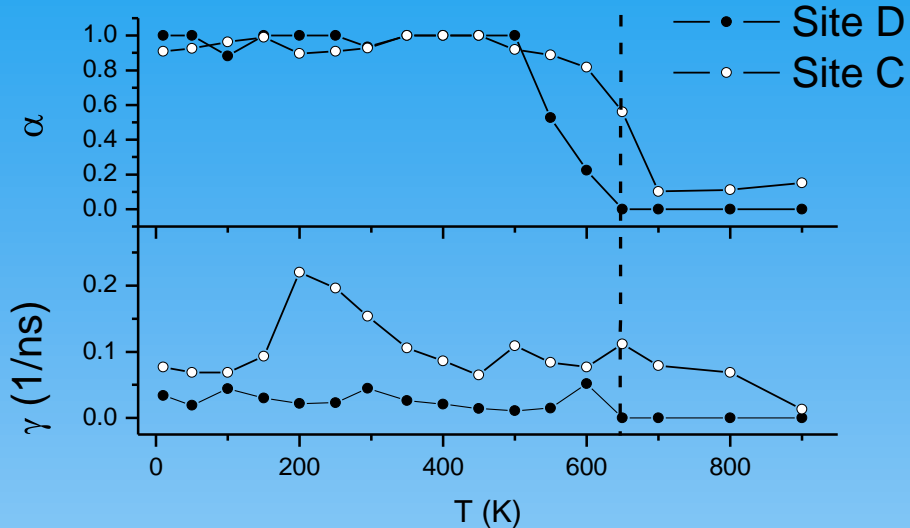
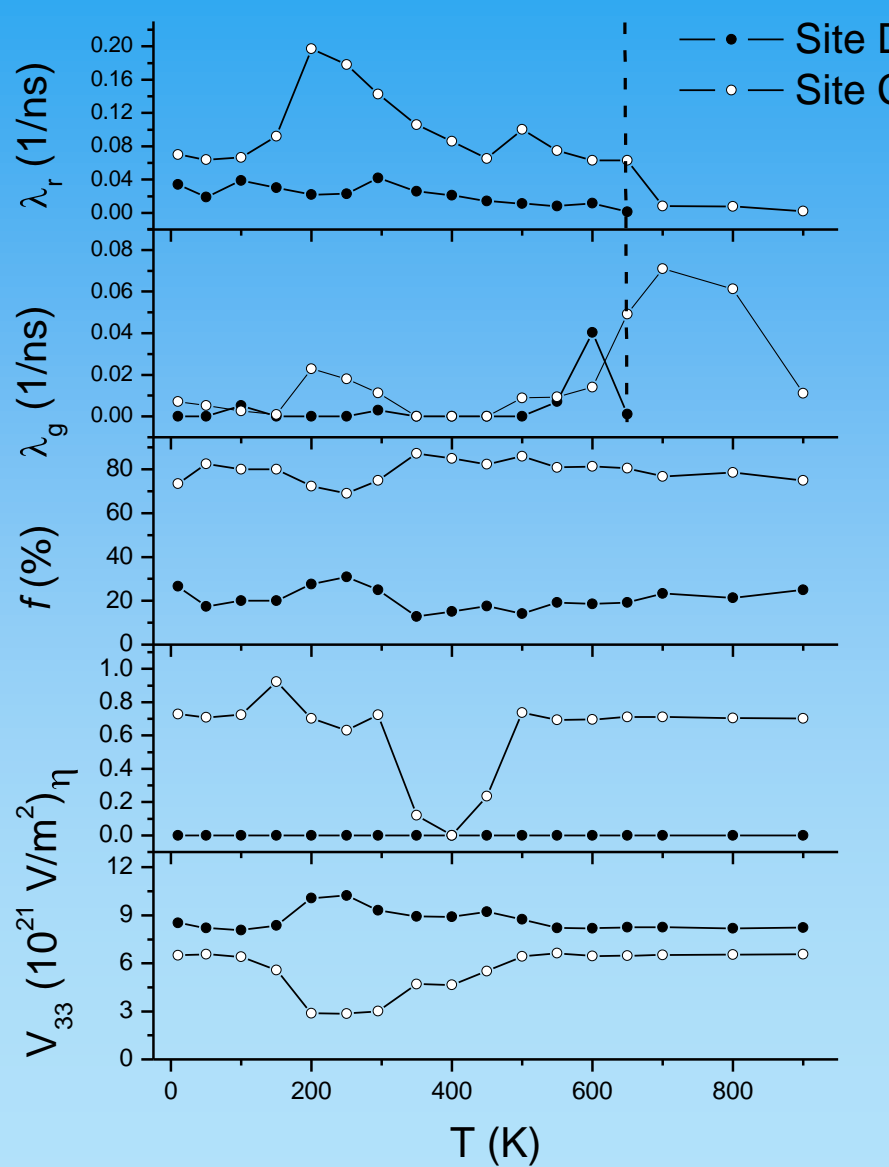


The PAC measurements reported by Bartos et al. [A. Bartos, et al., Phys. Lett. A **157**, 513 (1991)] do not present results of the HFI parameters vs. T.

Hyperfine Parameters vs. T



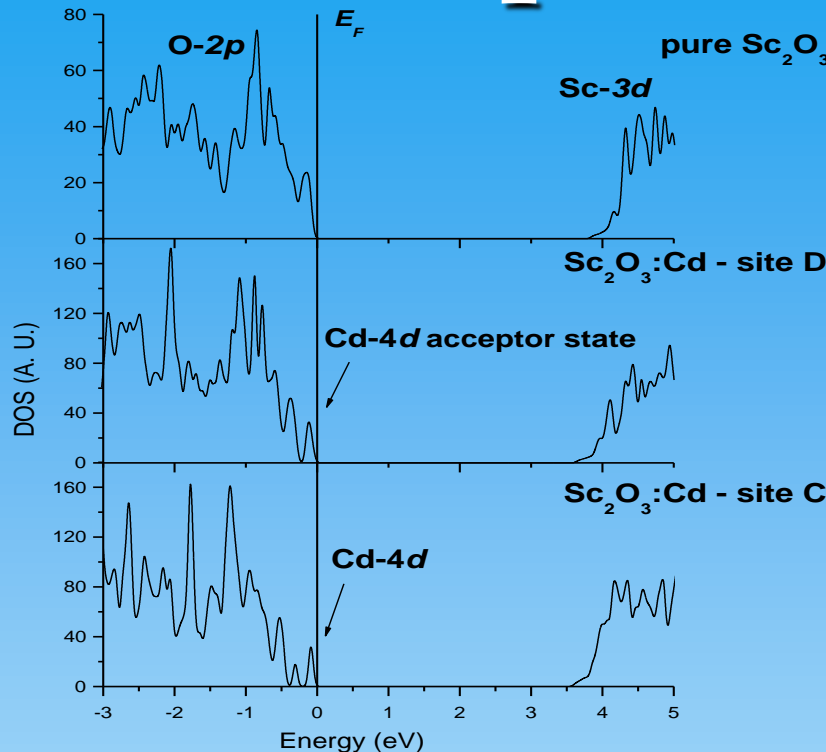
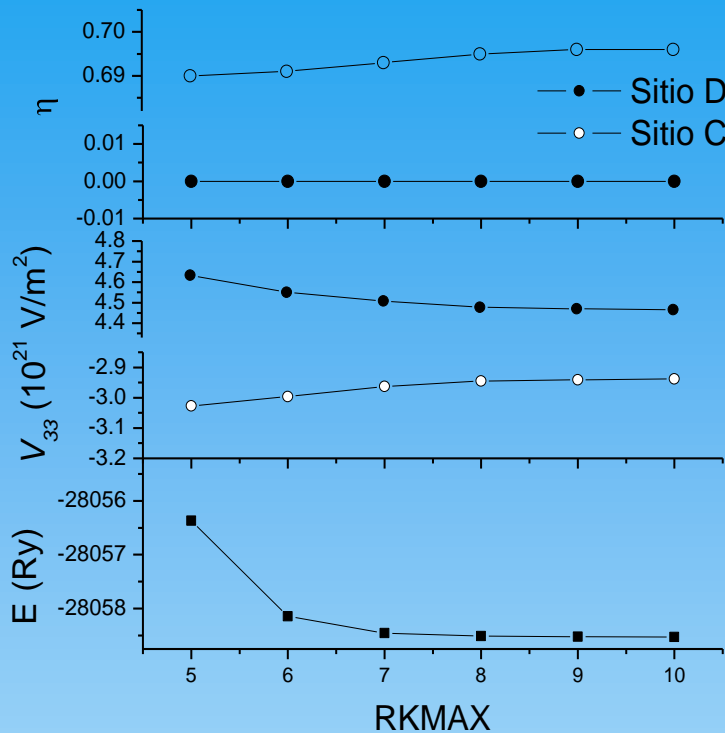
Hyperfine Parameters vs. T



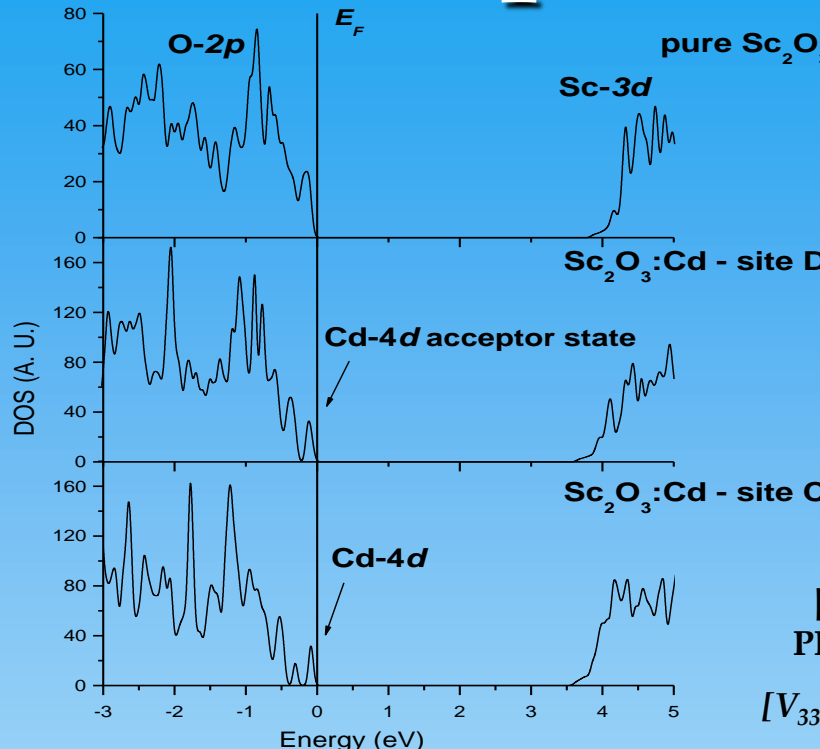
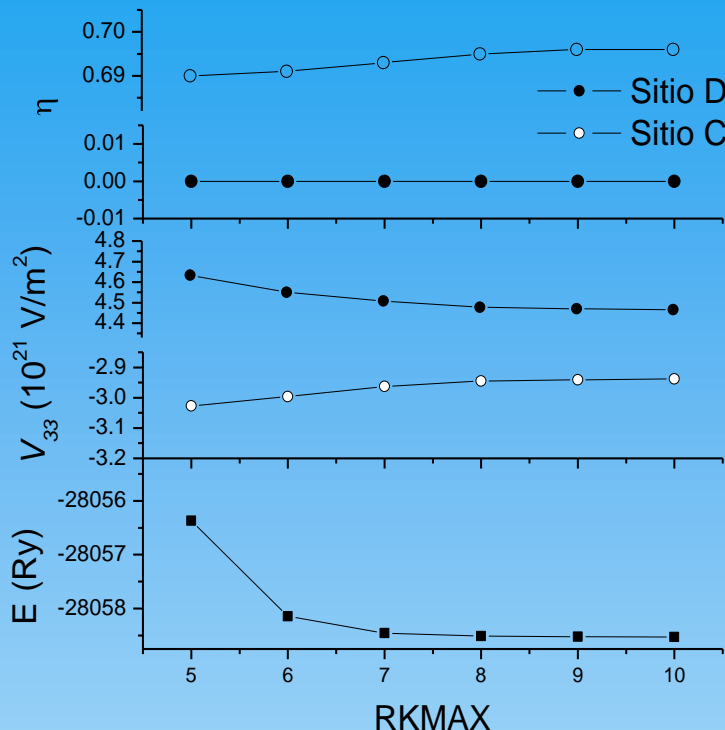
Outline

- Studied system
- PAC technique
- Experimental results
- FP-APW+lo calculations
- Final remarks

FP-APW+lo results in pure Sc_2O_3



FP-APW+lo results in pure Sc_2O_3



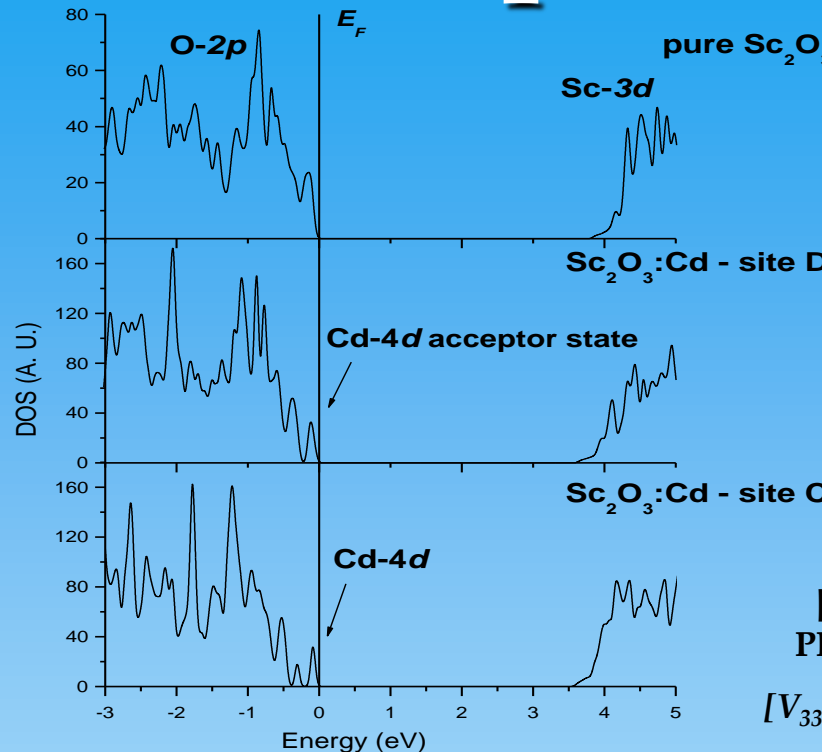
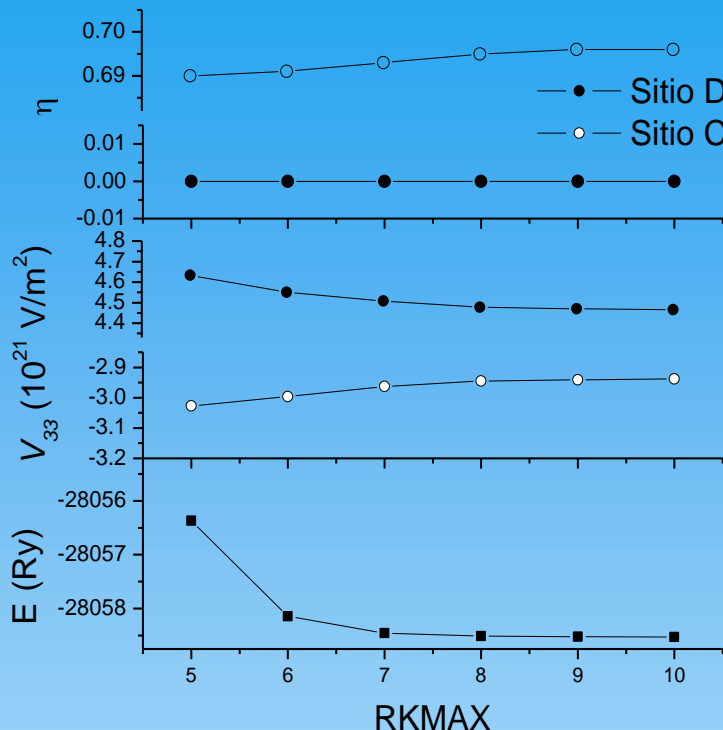
[1] D. Richard, et al.,
PRB 82, 035206 (2010).

$[V_{33}] = 10^{21} \text{ V/m}^2$; $[d_{NN}] = \text{\AA}$

Comparison between APW+lo results using experimental and refined structural parameters

Parameters	Aprox	Site D			Site C		
		d_{NN}	V_{33}	η	d_{NN}	V_{33}	η
Experimental	LDA	2.12	+4.53	0.00	2.08	-2.98	0.71
	CW	2.12	+4.52	0.00	2.08	-2.97	0.69
refined	LDA	2.12	+4.69	0.00	2.09	-3.11	0.53
	CW	2.12	+4.59	0.00	2.09	-2.92	0.52
PAC in ${}^{44}\text{Sc}$ results [1]			4.19(2)	0.00		2.741(7)	0.630(3)

FP-APW+lo results in pure Sc_2O_3



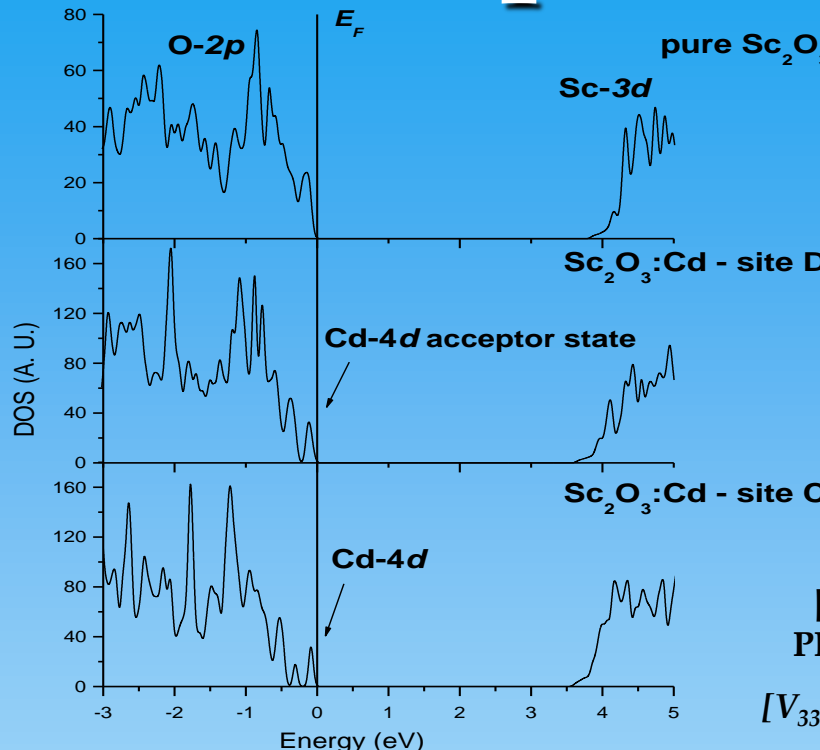
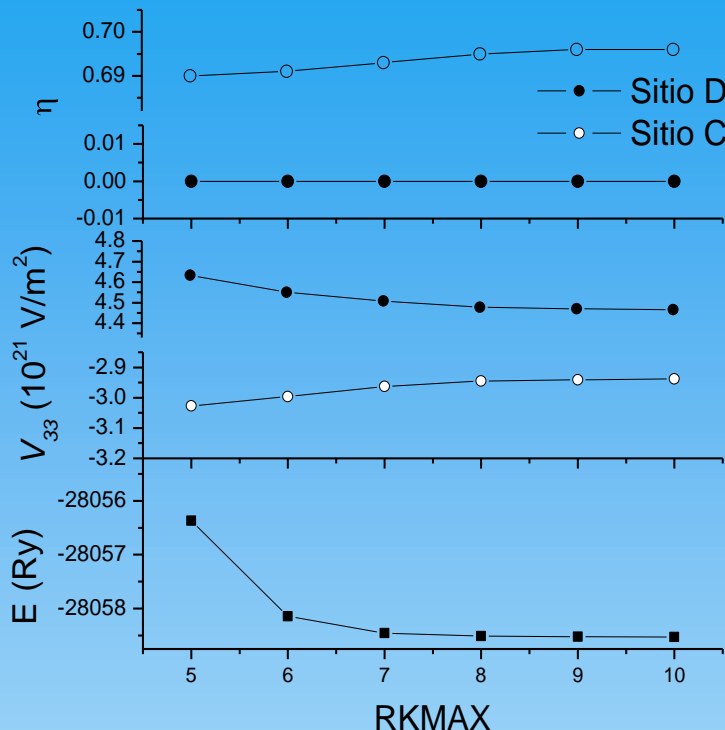
[1] D. Richard, et al.,
PRB 82, 035206 (2010).

$[V_{33}] = 10^{21} \text{ V/m}^2$; $[d_{NN}] = \text{\AA}$

Comparison between APW+lo results using experimental and refined structural parameters

Parameters	Aprox	Site D			Site C		
		d_{NN}	V_{33}	η	d_{NN}	V_{33}	η
Experimental	LDA	2.12	+4.53	0.00	2.08	-2.98	0.71
	CW	2.12	+4.52	0.00	2.08	-2.97	0.69
refined	LDA	2.12	+4.69	0.00	2.09	-3.11	0.53
	CW	2.12	+4.59	0.00	2.09	-2.92	0.52
PAC in ${}^{44}\text{Sc}$ results [1]			4.19(2)	0.00		2.741(7)	0.630(3)

FP-APW+lo results in pure Sc_2O_3



[1] D. Richard, et al.,
PRB 82, 035206 (2010).

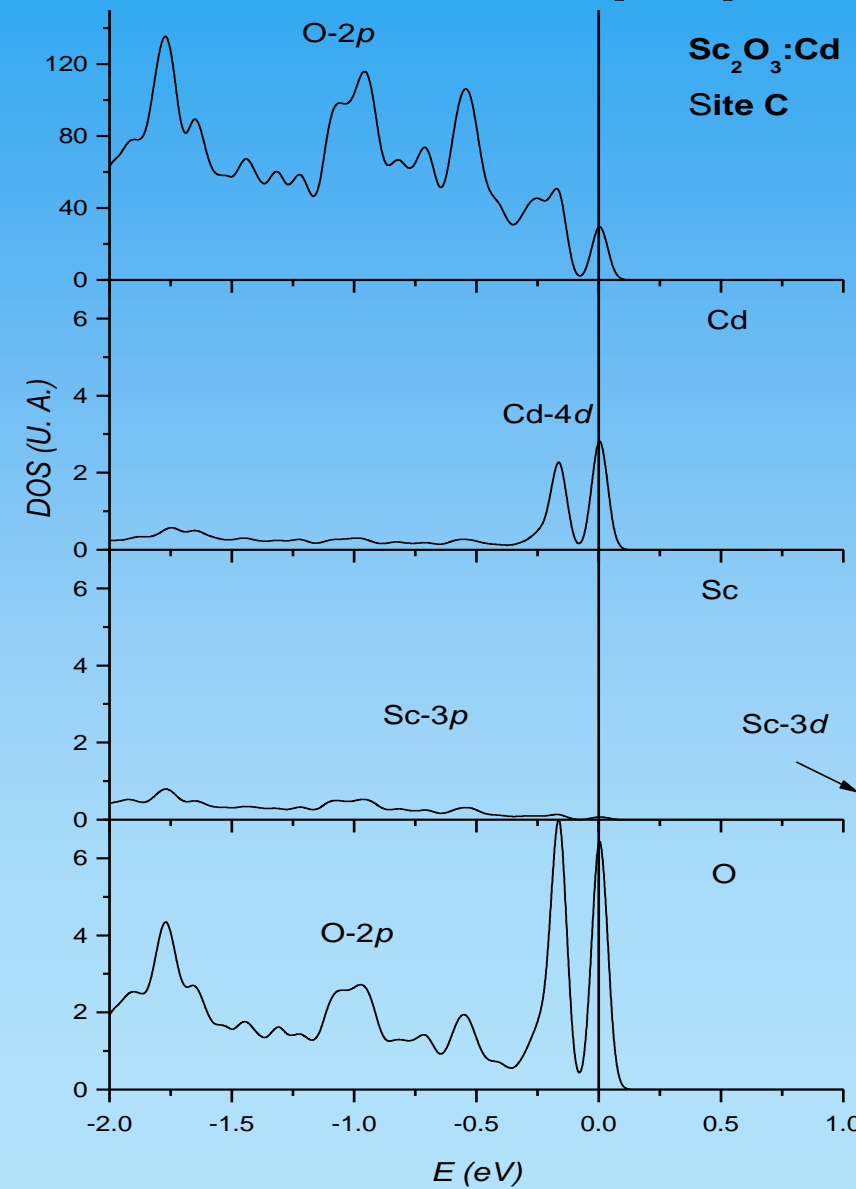
$[V_{33}] = 10^{21} \text{ V/m}^2$; $[d_{NN}] = \text{\AA}$

Comparison between APW+lo results using experimental and refined structural parameters

Parameters	Aprox	Site D			Site C		
		d_{NN}	V_{33}	η	d_{NN}	V_{33}	η
Experimental	LDA		+4.53	0.00	2.08	-2.98	0.71
	CW	2.12	+4.52	0.00	2.08	-2.97	0.69
refined	LDA	2.12	+4.69	0.00	2.09	-3.11	0.53
	CW	2.12	+4.59	0.00	2.09	-2.92	0.52
PAC in ${}^{44}\text{Sc}$ results [1]			4.19(2)	0.00		2.741(7)	0.630(3)

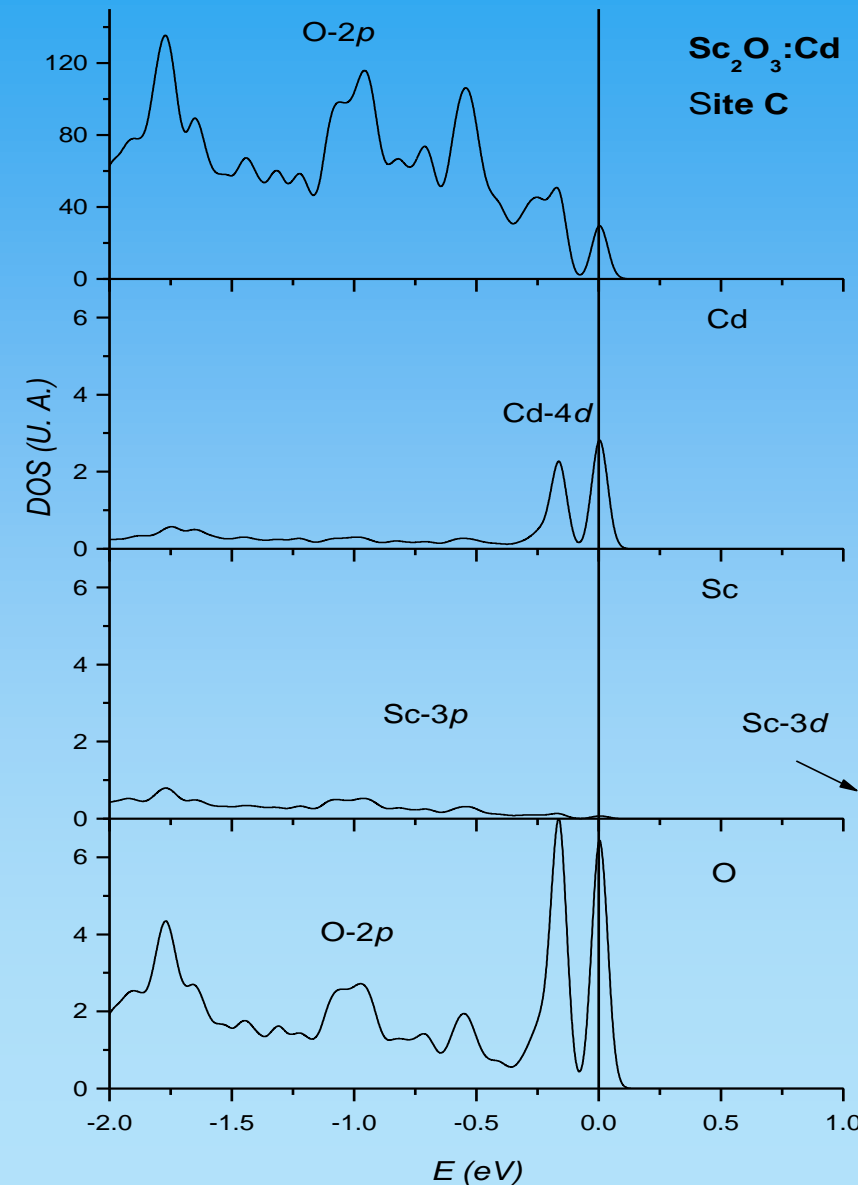
Total Density of States $\text{Sc}_2\text{O}_3:\text{Cd}$

Neutral cell (Cd^0)

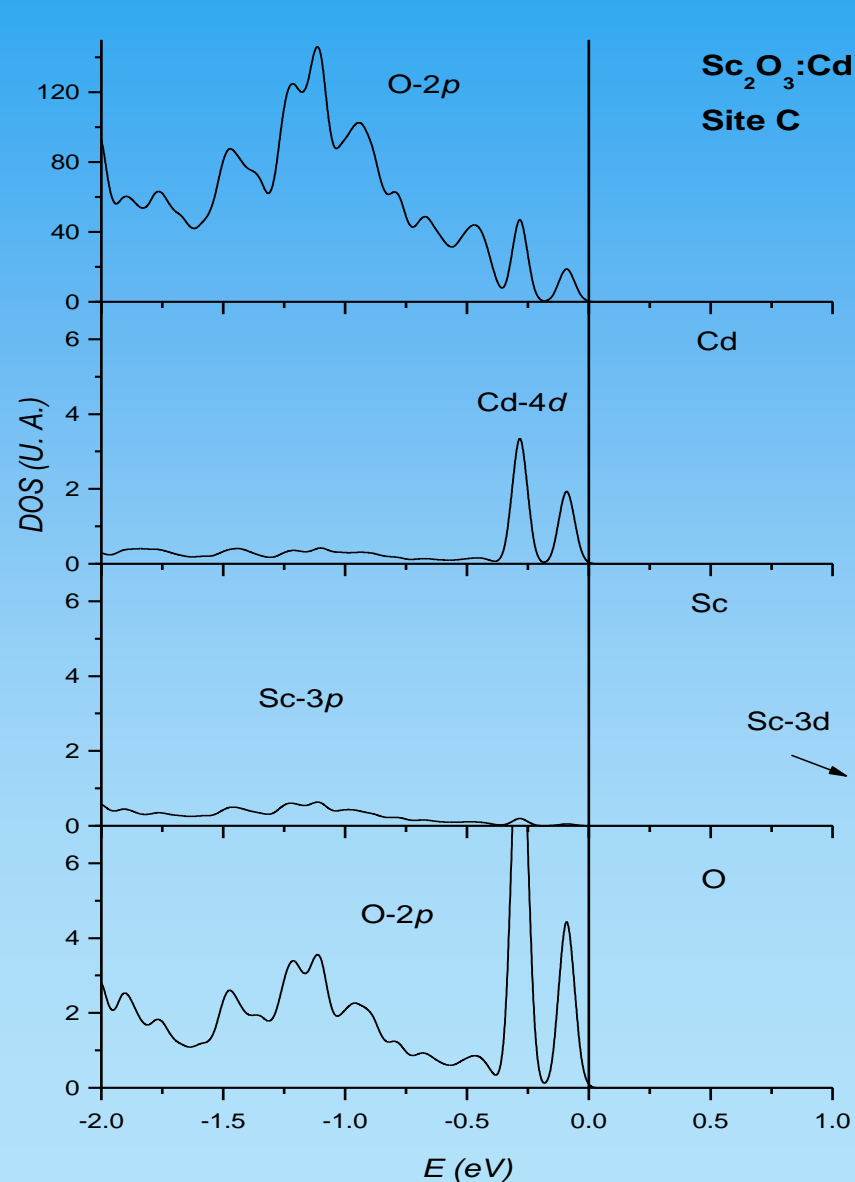


Total Density of States $\text{Sc}_2\text{O}_3:\text{Cd}$

Neutral cell (Cd^0)



Charged cell (Cd^{-1})



FP-APW+lo results in Cd-doped Sc_2O_3 for the unrelaxed and relaxed cell*

System	APW Approx.	Site D				Site C			
		d_{NN}	V_{33}	η	$\text{Dir. } V_{33}$	d_{NN}	V_{33}	η	$\text{Dir. } V_{33}$
Pure Sc_2O_3	LDA	2.12	4.63	0.0	[111]	2.08 2.12 2.16	-2.98 0.71	0.71	[0 -1 0.7]
Unrelaxed $\text{Sc}_2\text{O}_3:\text{Cd}$	LDA	2.12	8.65	0.0	[111]	2.08 2.12 2.16	-4.91 0.65	0.65	[0 -1 0.7]
Relaxed $\text{Sc}_2\text{O}_3:\text{Cd}$	LDA	2.28	8.05	0.0	[111]	2.17 2.30 2.31	6.75 0.74	0.74	[0 -0.9 1]
PAC results (T=900 K)			8.22₁	0.0	[111]	-	6.56₁	0.70₁	[0 -1 1]

* Cd-doped Sc_2O_3 results for the charged cell (Cd^{-1})

$[V_{33}] = 10^{21} \text{ V/m}^2$; $[d_{NN}] = \text{\AA}$

FP-APW+lo results in Cd-doped Sc_2O_3 for the unrelaxed and relaxed cell*

System	APW Approx.	Site D				Site C			
		d_{NN}	V_{33}	η	Dir. V_{33}	d_{NN}	V_{33}	η	Dir. V_{33}
Pure Sc_2O_3	LDA	2.12	4.63	0.0	[111]	2.08 2.12 2.16	-2.98	0.71	[0 -1 0.7]
Unrelaxed $\text{Sc}_2\text{O}_3:\text{Cd}$	LDA	2.12	8.65	0.0	[111]	2.08 2.12 2.16	-4.91	0.65	[0 -1 0.7]
Relaxed $\text{Sc}_2\text{O}_3:\text{Cd}$	LDA	2.28	8.05	0.0	[111]	2.17 2.30 2.31	6.75	0.74	[0 -0.9 1]
PAC results (T=900 K)		8.22₁	0.0	[111]	-	6.56 ₁	0.70 ₁	[0 -1 1]	

* Cd-doped Sc_2O_3 results for the charged cell (Cd^{-1})

$$[V_{33}] = 10^{21} \text{ V/m}^2; [d_{NN}] = \text{\AA}$$

FP-APW+lo results in Cd-doped Sc_2O_3 for the unrelaxed and relaxed cell*

System	APW Approx.	Site D				Site C			
		d_{NN}	V_{33}	η	$Dir. V_{33}$	d_{NN}	V_{33}	η	$Dir. V_{33}$
Pure Sc_2O_3	LDA	2.12	4.63	0.0	[111]	2.08 2.12 2.16	-2.98 0.71 [0 -1 0.7]	0.71 [0 -1 0.7]	
Unrelaxed $\text{Sc}_2\text{O}_3:\text{Cd}$	LDA	2.12	8.65	0.0	[111]	2.08 2.12 2.16	-4.91 0.65 [0 -1 0.7]	0.65 [0 -1 0.7]	
Relaxed $\text{Sc}_2\text{O}_3:\text{Cd}$	LDA	2.28	8.05	0.0	[111]	2.17 2.30 2.31	6.75 0.74 [0 -0.9 1]	0.74 [0 -0.9 1]	
PAC results (T=900 K)			8.22 ₁	0.0	[111]	-	6.56 ₁ 0.70 ₁	0.70 ₁	[0 -1 1]

* Cd-doped Sc_2O_3 results for the charged cell (Cd^{-1})

$$[V_{33}] = 10^{21} \text{ V/m}^2; [d_{NN}] = \text{\AA}$$

EFG dependence of the charge state of the Cd impurity

Cell Charge State	APW Appro	Site D					Site C				
		x.	d_{NN}	V_{33}	η	$Dir. V_{33}$	d_{NN}	V_{33}	η	$Dir. V_{33}$	
Uncharged Cell	WC	2.22	+8.24	0.00	[111]	2.10 2.24 2.32	2.24 2.28 2.32	+3.06	0.64	[0 0 1]	
Neutral Cell	WC	2.25	+8.32	0.00	[111]	2.14 2.28 2.32	2.28 2.32	-3.81	0.34	[0 -0.7 1]	
Charged Cell	WC	2.28	+8.16	0.00	[111]	2.19 2.31 2.32	2.31 2.32	+6.50	0.71	[0 -0.8 1]	

These results were checked with the others approximations, LDA and GGA
 $[V_{33}] = 10^{21} \text{ V/m}^2$; $[d_{NN}] = \text{\AA}$

Uncharged cell (Cd^{+1}): 1 removed electron in the cell

Neutral cell (Cd^0): neutral Cd atom

Charged cell (Cd^{-1}): 1 added electron in the cell

EFG dependence of the charge state of the Cd impurity

Cell Charge State	APW Appro.	Site D				Site C			
		d_{NN}	V_{33}	η	$Dir. V_{33}$	d_{NN}	V_{33}	η	$Dir. V_{33}$
Uncharged Cell	WC	2.22	+8.24	0.00	[111]	2.10 2.24 2.32	+3.06 -3.81 2.32	0.64 0.34	[0 0 1]
Neutral Cell	WC	2.25	+8.32	0.00	[111]	2.14 2.28 2.32	-3.81 +6.50	0.34 0.71	[0 -0.7 1]
Charged Cell	WC	2.28	+8.16	0.00	[111]	2.19 2.31 2.32			[0 -0.8 1]

These results were checked with the others approximations, LDA and GGA
 $[V_{33}] = 10^{21} \text{ V/m}^2$; $[d_{NN}] = \text{\AA}$

Uncharged cell (Cd^{+1}): 1 removed electron in the cell

Neutral cell (Cd^0): neutral Cd atom

Charged cell (Cd^{-1}): 1 added electron in the cell

EFG dependence of the charge state of the Cd impurity

Cell Charge State	APW Appro	Site D					Site C				
		x.	d_{NN}	V_{33}	η	<i>Dir.</i> V_{33}	d_{NN}	V_{33}	η	<i>Dir.</i> V_{33}	
Uncharged Cell	WC	2.22	+8.24	0.00	[111]		2.10 2.24 2.32	+3.06 -3.81 2.32	0.64 0.34	[0 0 1]	
Neutral Cell	WC	2.25	+8.32	0.00	[111]		2.14 2.28 2.32	-3.81 +6.50	0.34 0.71	[0 -0.7 1]	
Charged Cell	WC	2.28	+8.16	0.00	[111]		2.19 2.31 2.32			[0 -0.8 1]	

These results were checked with the others approximations, LDA and GGA
 $[V_{33}] = 10^{21} \text{ V/m}^2$; $[d_{NN}] = \text{\AA}$

Uncharged cell (Cd^{+1}): 1 removed electron in the cell

Neutral cell (Cd^0): neutral Cd atom

Charged cell (Cd^{-1}): 1 added electron in the cell

EFG contributions

Cd at D site									
	Uncharged Cell			Neutral Cell			Charged Cell		
	V_{11}	V_{22}	V_{33}	V_{11}	V_{22}	V_{33}	V_{11}	V_{22}	V_{33}
p	-3.34	-3.34	6.68	-3.18	-3.18	6.36	-3.00	-3.00	6.00
d	-0.89	-0.89	1.78	-1.08	-1.08	2.16	-1.17	-1.17	2.35
s-d	0.10	0.10	-0.20	0.10	0.10	-0.20	0.10	0.10	-0.20
total	-4.13	-4.13	8.26	-4.16	-4.16	8.32	-4.07	-4.07	8.15

$[V_{ii}] = 10^{21} \text{ V/m}^2$

EFG contributions

Cd at D site									
	Uncharged Cell			Neutral Cell			Charged Cell		
	V_{11}	V_{22}	V_{33}	V_{11}	V_{22}	V_{33}	V_{11}	V_{22}	V_{33}
p	-3.34	-3.34	6.68	-3.18	-3.18	6.36	-3.00	-3.00	6.00
d	-0.89	-0.89	1.78	-1.08	-1.08	2.16	-1.17	-1.17	2.35
s-d	0.10	0.10	-0.20	0.10	0.10	-0.20	0.10	0.10	-0.20
total	-4.13	-4.13	8.26	-4.16	-4.16	8.32	-4.07	-4.07	8.15

$[V_{ii}] = 10^{21} \text{ V/m}^2$

EFG contributions

Cd at D site									
	Uncharged Cell			Neutral Cell			Charged Cell		
	\mathbf{V}_{11}	\mathbf{V}_{22}	\mathbf{V}_{33}	\mathbf{V}_{11}	\mathbf{V}_{22}	\mathbf{V}_{33}	\mathbf{V}_{11}	\mathbf{V}_{22}	\mathbf{V}_{33}
p	-3.34	-3.34	6.68	-3.18	-3.18	6.36	-3.00	-3.00	6.00
d	-0.89	-0.89	1.78	-1.08	-1.08	2.16	-1.17	-1.17	2.35
s-d	0.10	0.10	-0.20	0.10	0.10	-0.20	0.10	0.10	-0.20
total	-4.13	-4.13	8.26	-4.16	-4.16	8.32	-4.07	-4.07	8.15
Cd at C site									
	Uncharged Cell			Neutral Cell			Charged Cell		
	\mathbf{V}_{11}	\mathbf{V}_{22}	\mathbf{V}_{33}	\mathbf{V}_{11}	\mathbf{V}_{22}	\mathbf{V}_{33}	\mathbf{V}_{11}	\mathbf{V}_{22}	\mathbf{V}_{33}
p	9.60	-6.47	-3.12	-2.24	7.46	-5.22	-1.20	-3.67	4.87
d	-10.32	4.20	6.12	3.46	-4.86	1.39	0.25	-2.03	1.78
s-d	0.17	-0.21	0.05	0.04	0.15	-0.19	0.02	0.13	-0.15
total	-0.5	-2.53	3.03	1.25	2.57	-3.82	-0.93	-5.57	6.50

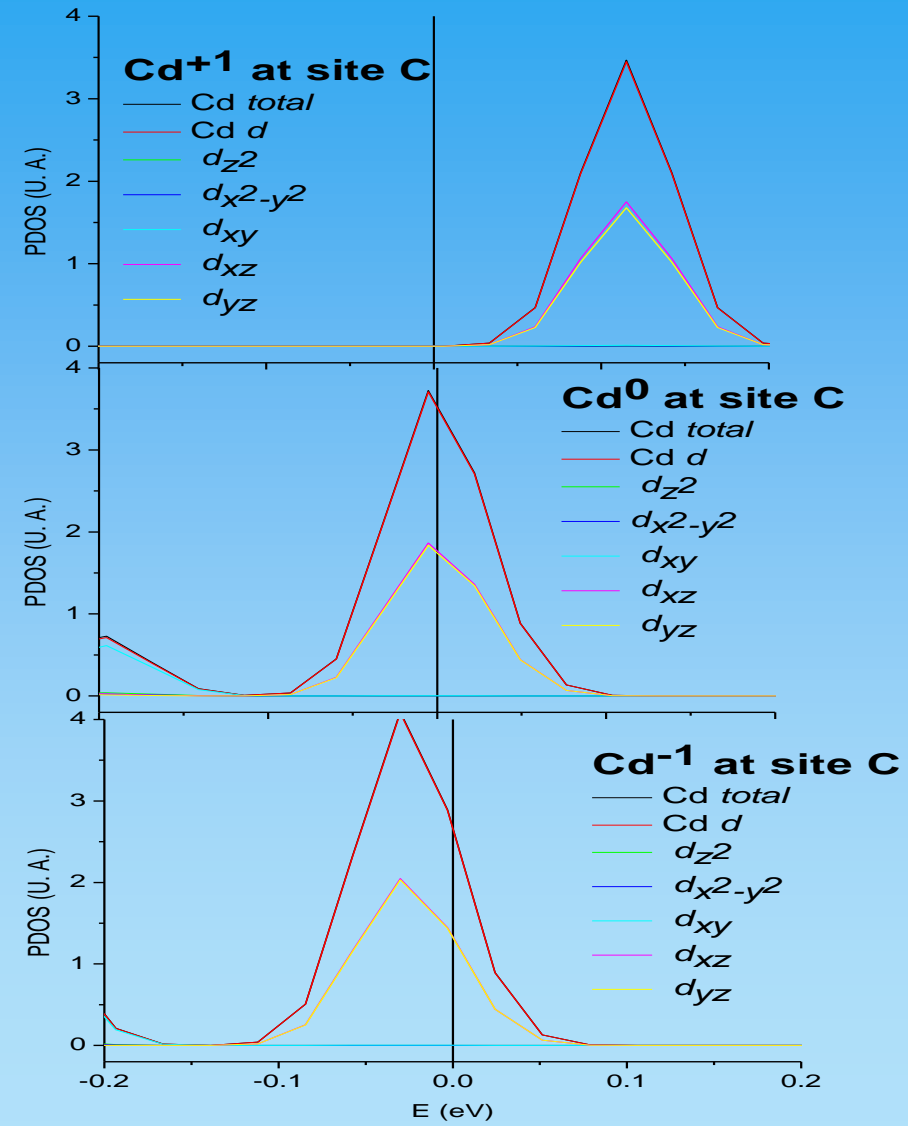
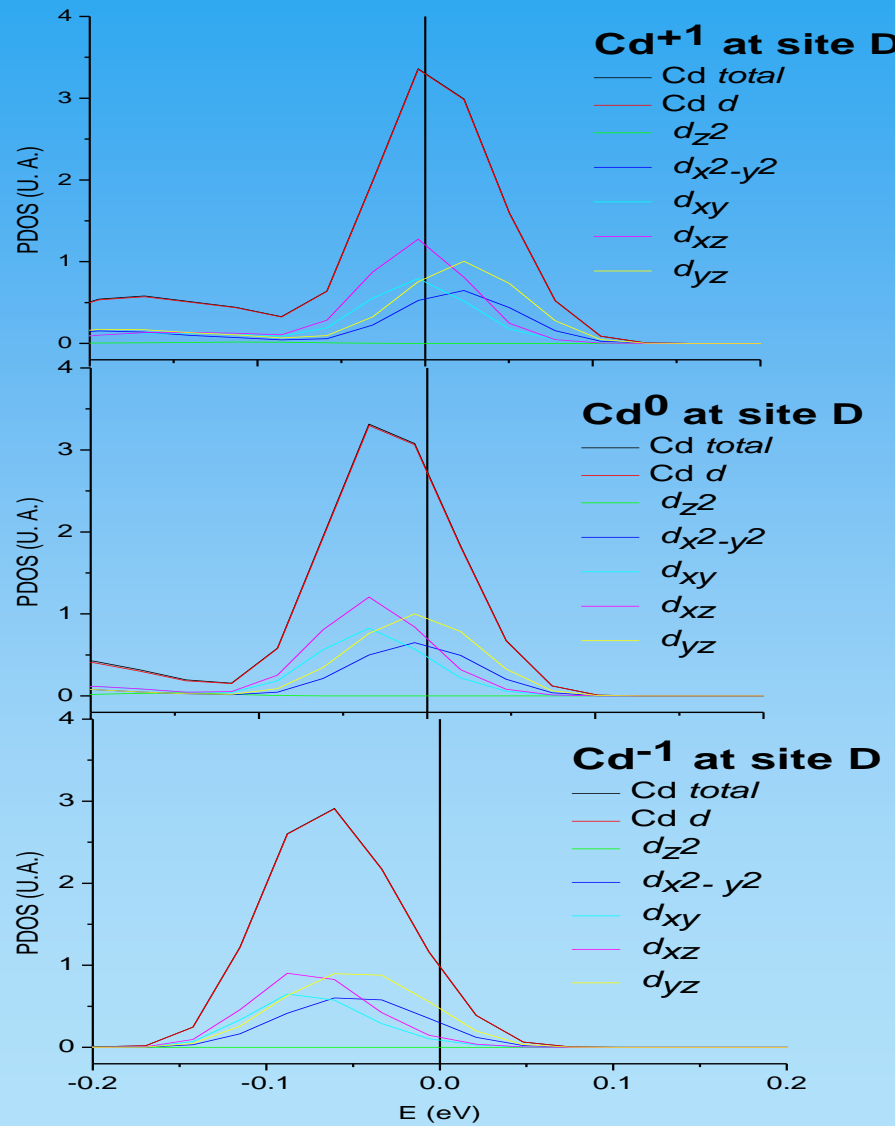
[V_{ii}]= 10^{21} V/m²

EFG contributions

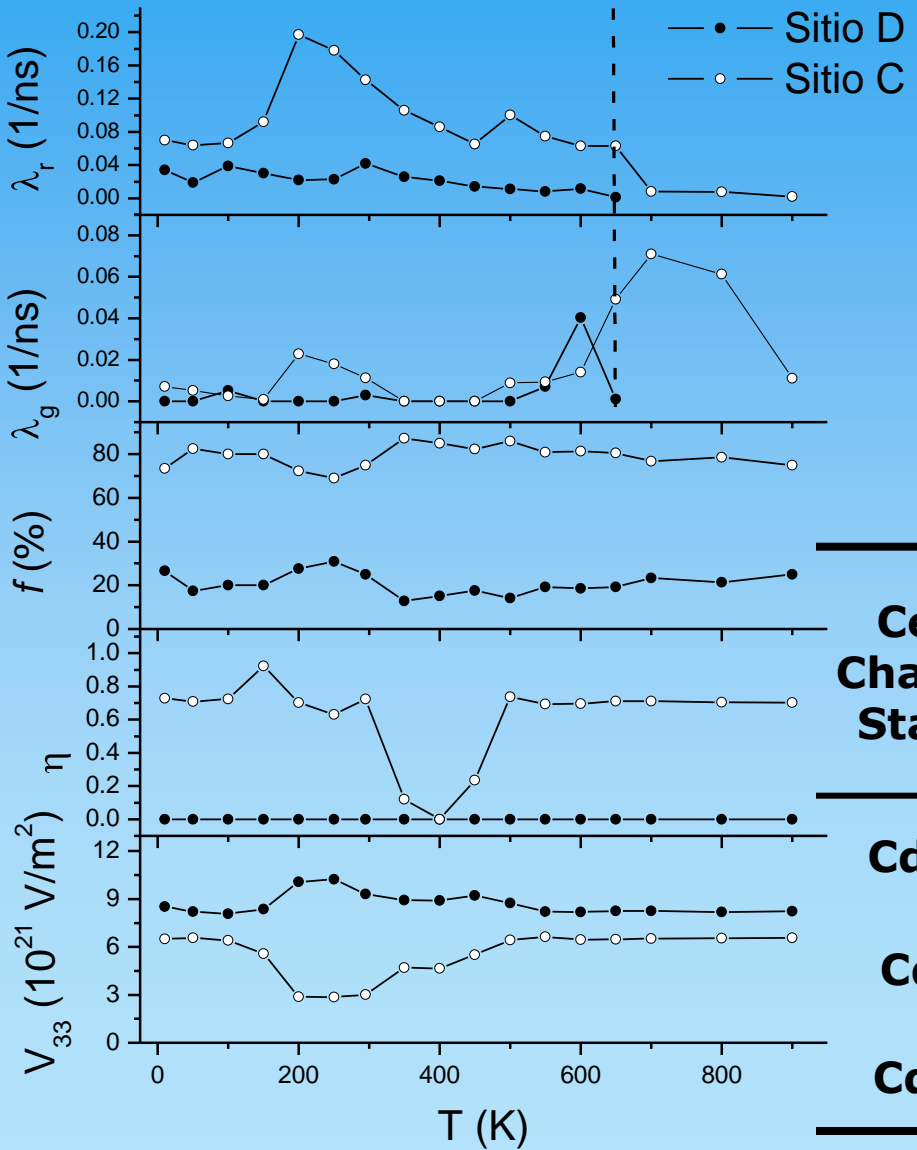
Cd at D site									
	Uncharged Cell			Neutral Cell			Charged Cell		
	V_{11}	V_{22}	V_{33}	V_{11}	V_{22}	V_{33}	V_{11}	V_{22}	V_{33}
p	-3.34	-3.34	6.68	-3.18	-3.18	6.36	-3.00	-3.00	6.00
d	-0.89	-0.89	1.78	-1.08	-1.08	2.16	-1.17	-1.17	2.35
s-d	0.10	0.10	-0.20	0.10	0.10	-0.20	0.10	0.10	-0.20
total	-4.13	-4.13	8.26	-4.16	-4.16	8.32	-4.07	-4.07	8.15
Cd at C site									
	Uncharged Cell			Neutral Cell			Charged Cell		
	V_{11}	V_{22}	V_{33}	V_{11}	V_{22}	V_{33}	V_{11}	V_{22}	V_{33}
p	9.60	-6.47	-3.12	-2.24	7.46	-5.22	-1.20	-3.67	4.87
d	-10.32	4.20	6.12	3.46	-4.86	1.39	0.25	-2.03	1.78
s-d	0.17	-0.21	0.05	0.04	0.15	-0.19	0.02	0.13	-0.15
total	-0.5	-2.53	3.03	1.25	2.57	-3.82	-0.93	-5.57	6.50

$[V_{ii}] = 10^{21} \text{ V/m}^2$

Partial Density of States Cd-4d



Comparison of the results



**Cell
Charge
State**

**APW
Approx.**

Cd⁺¹

Cd⁰

Cd⁻¹

Site D

Site C

V_{33}

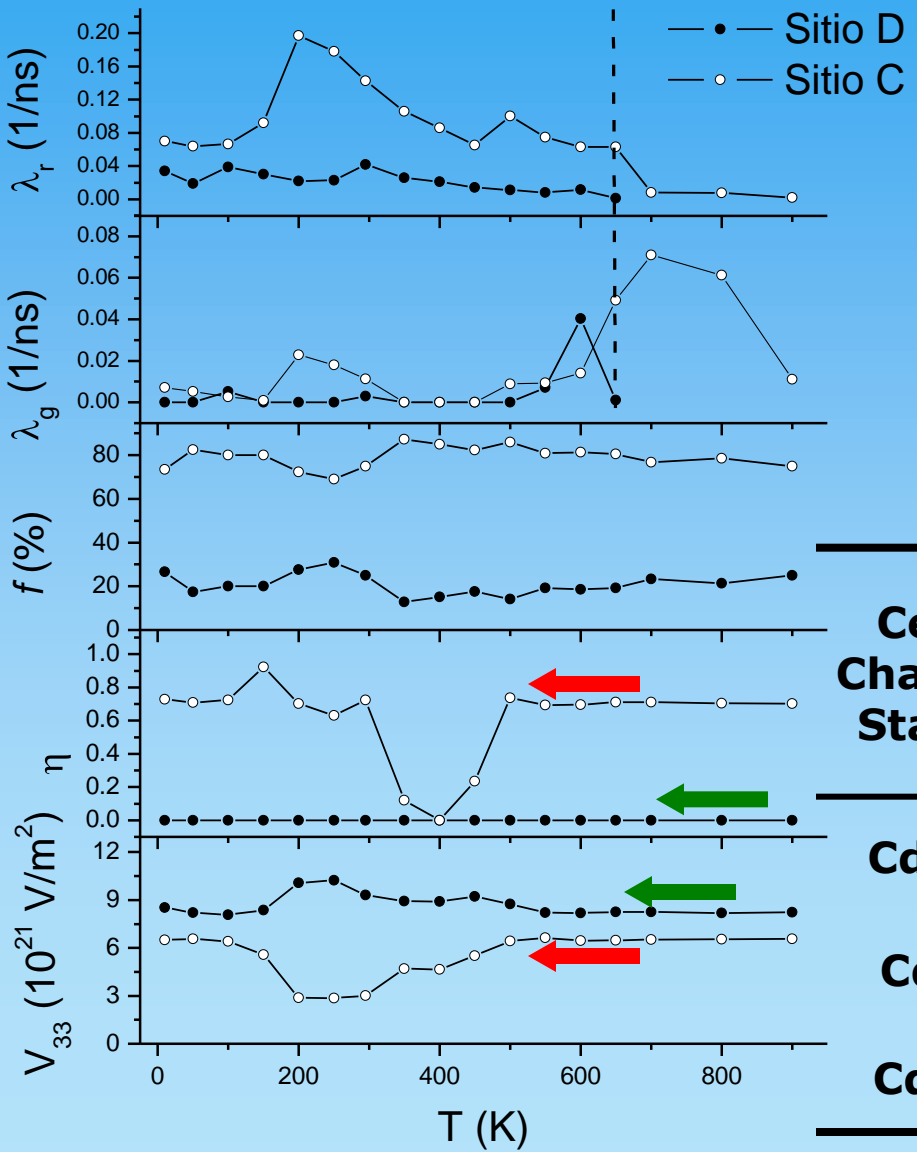
η

V_{33}

η

WC-GGA	+8.24	0.00	+3.06	0.64
WC-GGA	+8.32	0.00	-3.81	0.34
WC-GGA	+8.16	0.00	+6.50	0.71

Comparison of the results



**Cell
Charge
State**

**APW
Approx.**

Cd⁺¹

Cd⁰

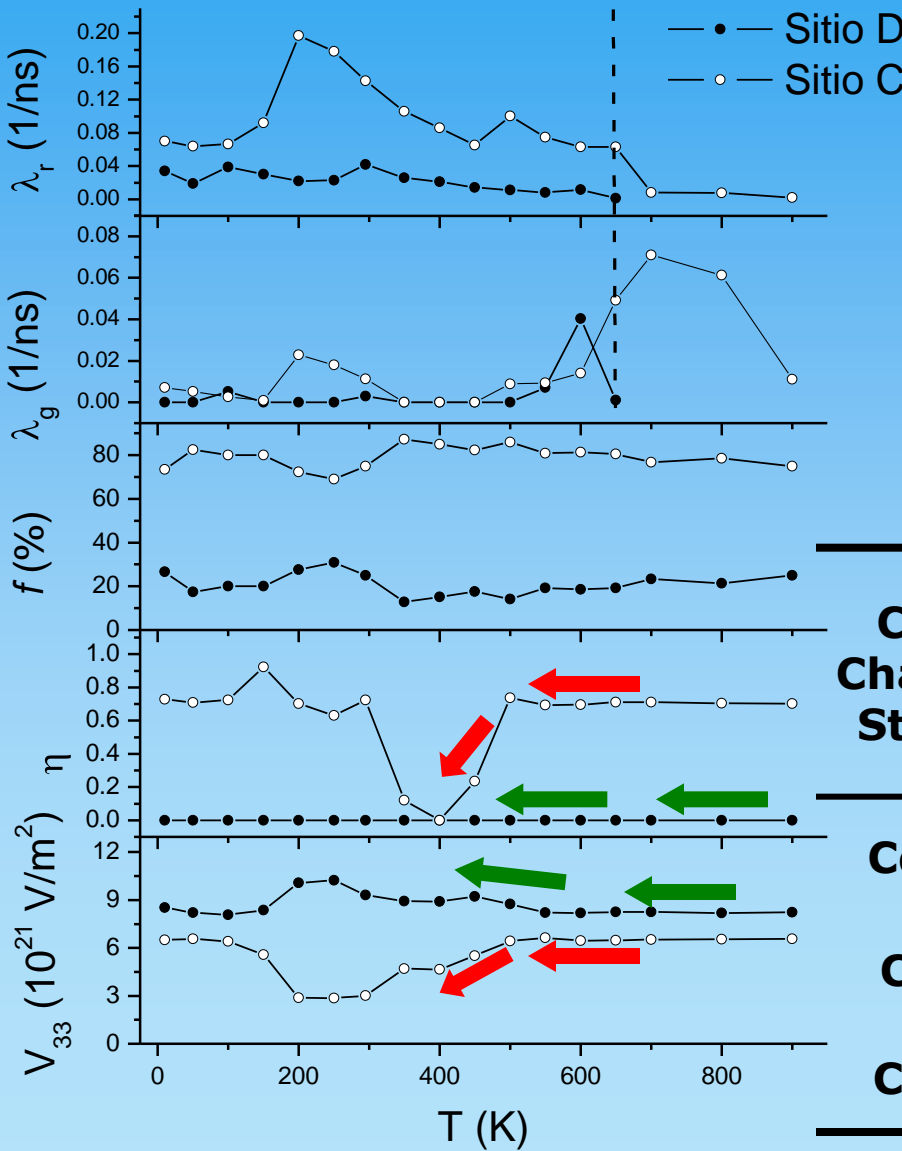
Cd⁻¹

Site D

Site C

		V_{33}	η	V_{33}	η
Cd⁺¹	WC-GGA	+8.24	0.00	+3.06	0.64
Cd⁰	WC-GGA	+8.32	0.00	-3.81	0.34
Cd⁻¹	WC-GGA	+8.16	0.0	+6.50	0.71

Comparison of the results



**Cell
Charge
State**

**APW
Approx.**

Cd^{+1}

WC-GGA

V_{33}

η

Site D

V_{33}

η

Cd^0

WC-GGA

V_{33}

η

Cd^{-1}

WC-GGA

V_{33}

η

+8.24

0.00

+3.06

0.64

+8.32

0.0

-3.81

0.34

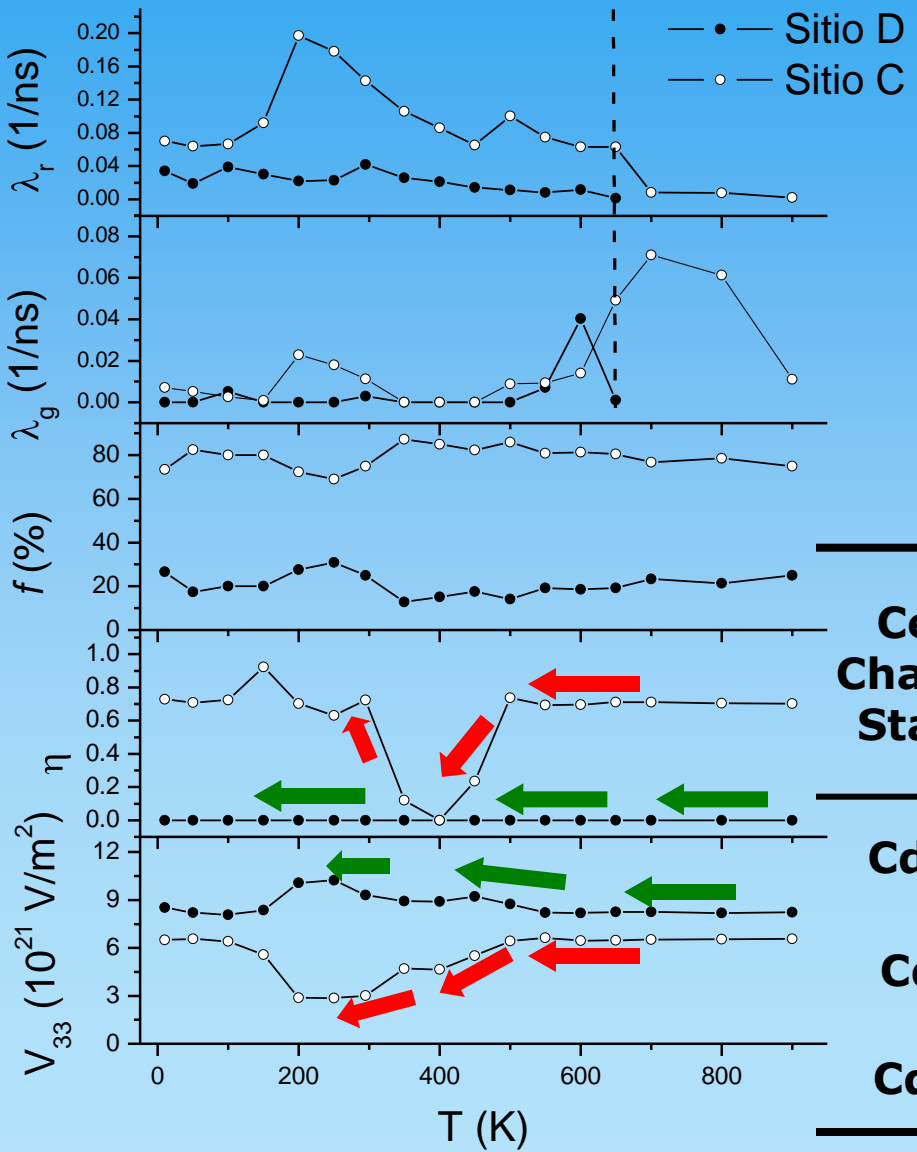
+8.16

0.0

+6.50

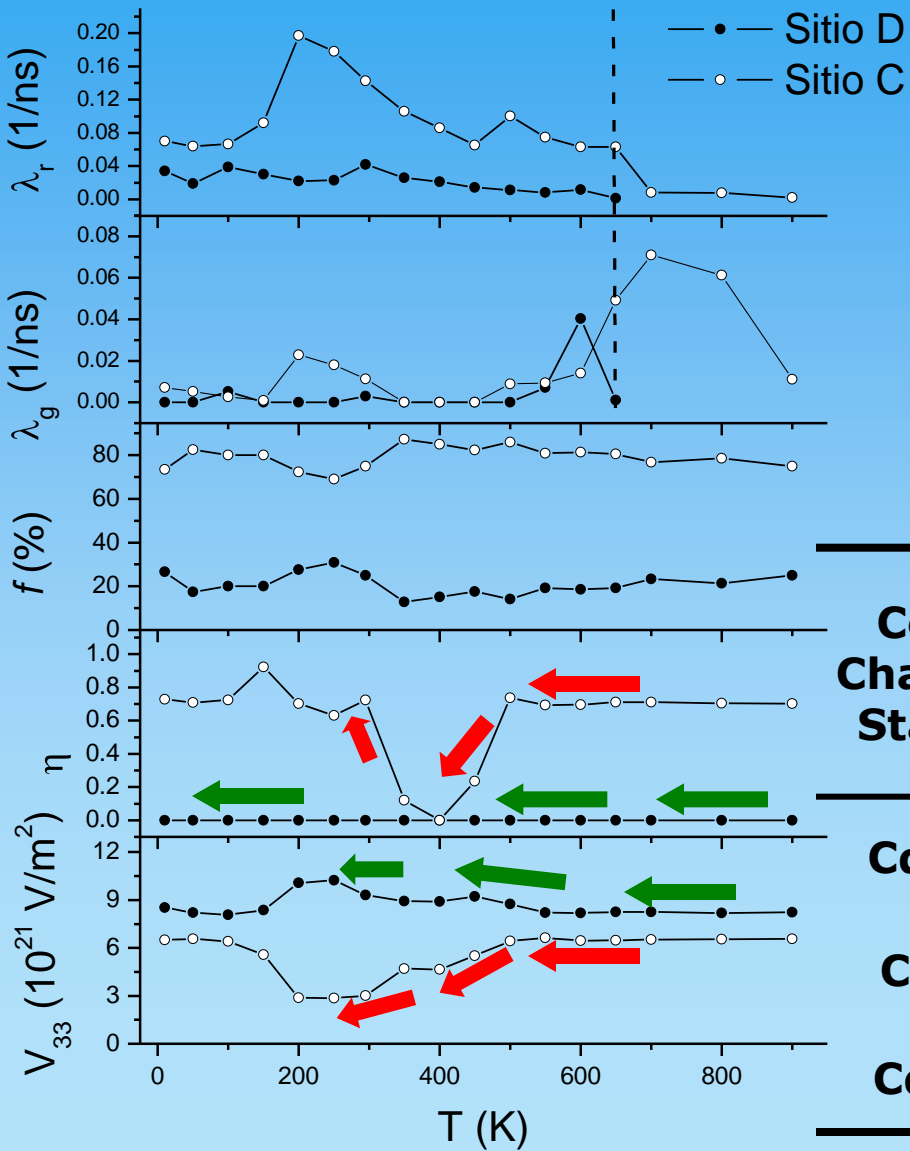
0.71

Comparison of the results



Cell Charge State	APW Approx.	Site D		Site C	
		V_{33}	η	V_{33}	η
Cd^{+1}	WC-GGA	+8.24	0.0	+3.06	0.64
Cd^0	WC-GGA	+8.32	0.0	-3.81	0.34
Cd^{-1}	WC-GGA	+8.16	0.0	+6.50	0.71

Comparison of the results



Cell Charge State	APW Approx.	Site D		Site C	
		V_{33}	η	V_{33}	η
Cd^{+1}	WC-GGA	+8.24	0.0	+3.06	0.64
Cd^0	WC-GGA	+8.32	0.0	-3.81	0.34
Cd^{-1}	WC-GGA	+8.16	0.0	+6.50	0.71

Outline

- Studied system
- PAC technique
- Experimental results
- FP-APW+lo calculations
- Final remarks

Final remarks

- From this experimental and *ab initio* approach, we can conclude that the dynamic interaction observed at Cd impurities located at C sites is more intense than the dynamic interaction at the D site. These behavior of the EFG is attributed to the symmetry of the each site.

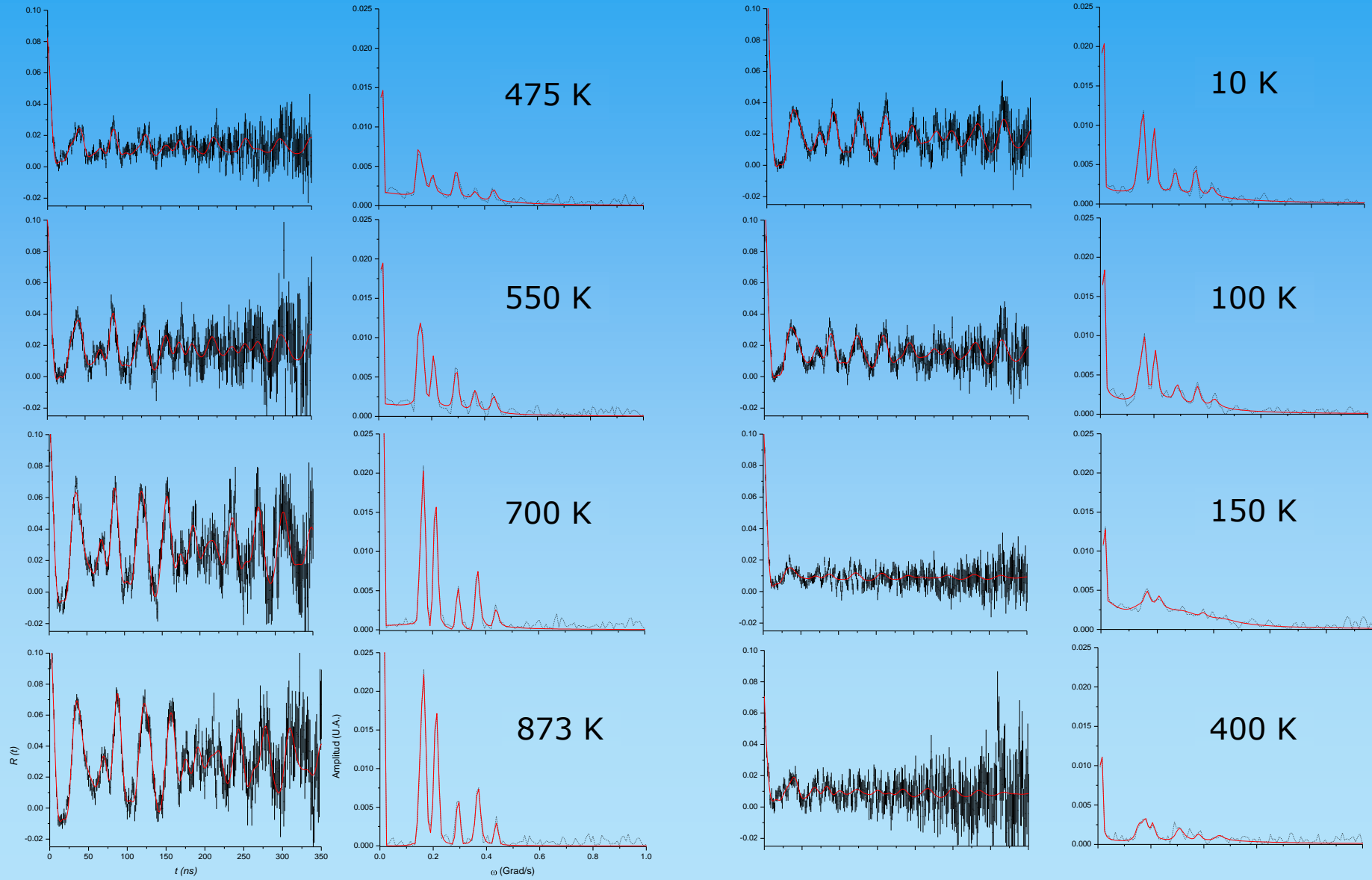
Final remarks

- From this experimental and *ab initio* approach, we can conclude that the dynamic interaction observed at Cd impurities located at C sites is more intense than the dynamic interaction at the D site. These behavior of the EFG is attributed to the symmetry of the each site.
- We can see that the increase of the EFG dependence with the charge state of the impurity is correlated with an increase of the strength of the dynamic interaction.

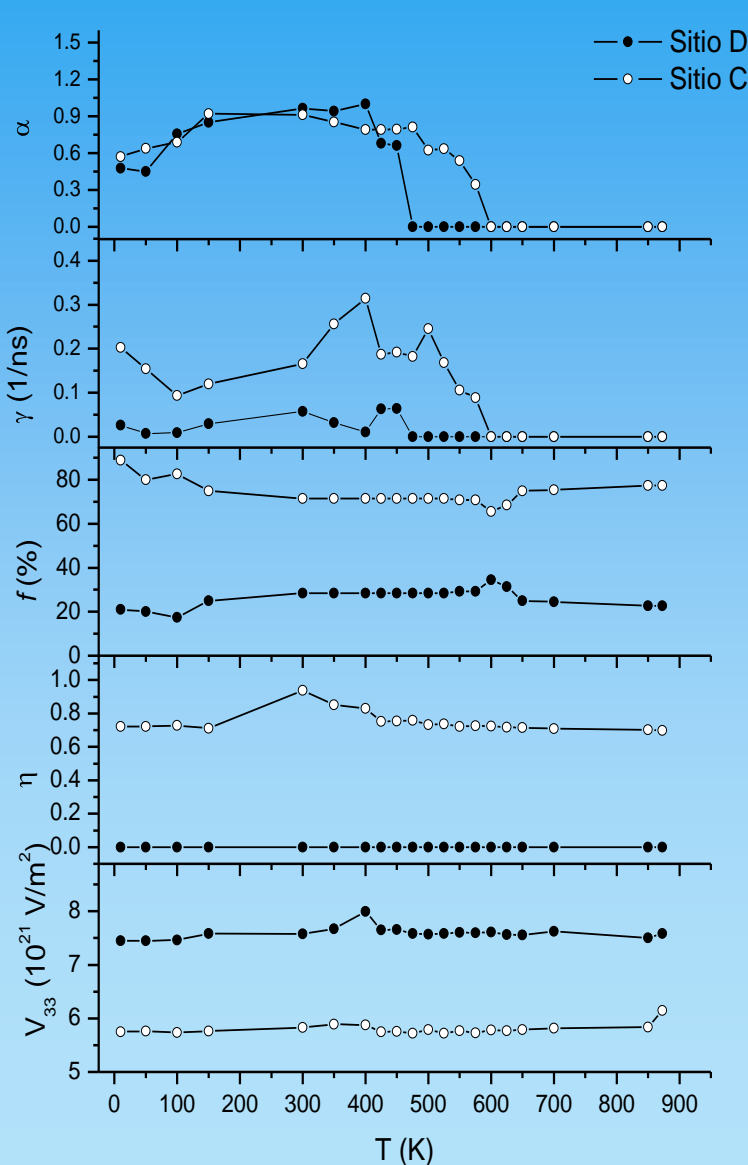
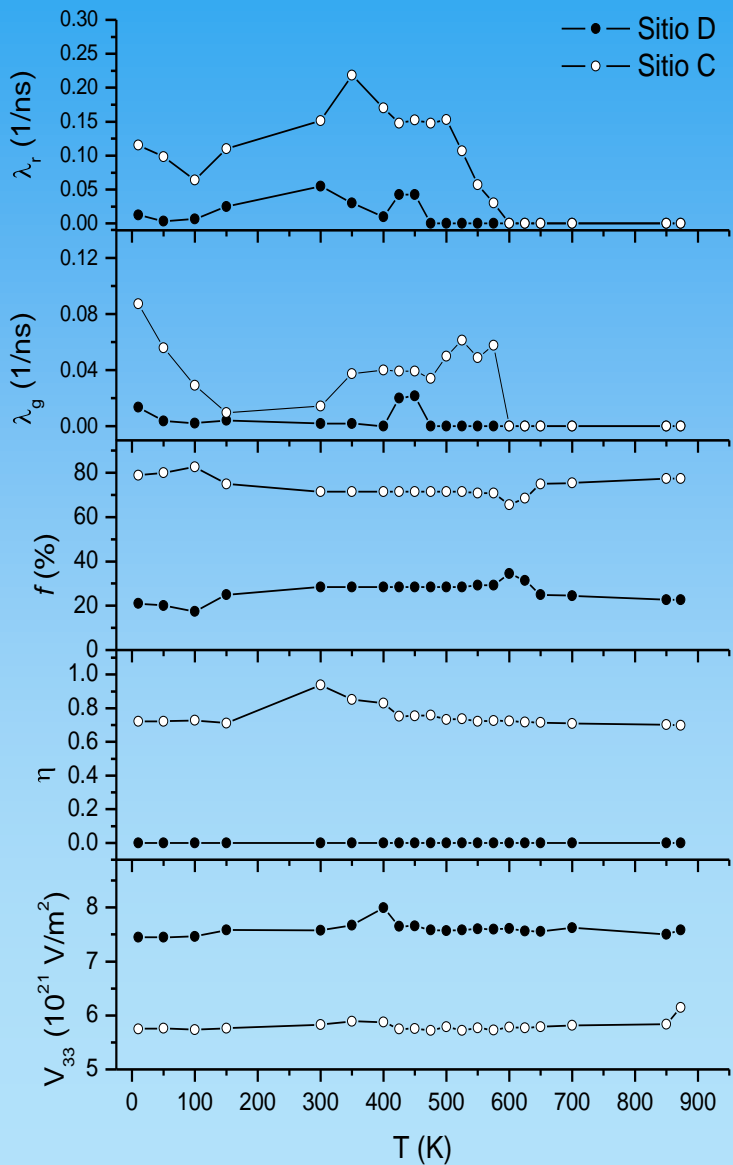
Final remarks

- From this experimental and *ab initio* approach, we can conclude that the dynamic interaction observed at Cd impurities located at C sites is more intense than the dynamic interaction at the D site. These behavior of the EFG is attributed to the symmetry of the each site.
- We can see that the increase of the EFG dependence with the charge state of the impurity is correlated with an increase of the strength of the dynamic interaction.
- Finally, we conclude that an *ab initio* study can help to understand the underlying physics described by the phenomenological Abragam and Pound model.

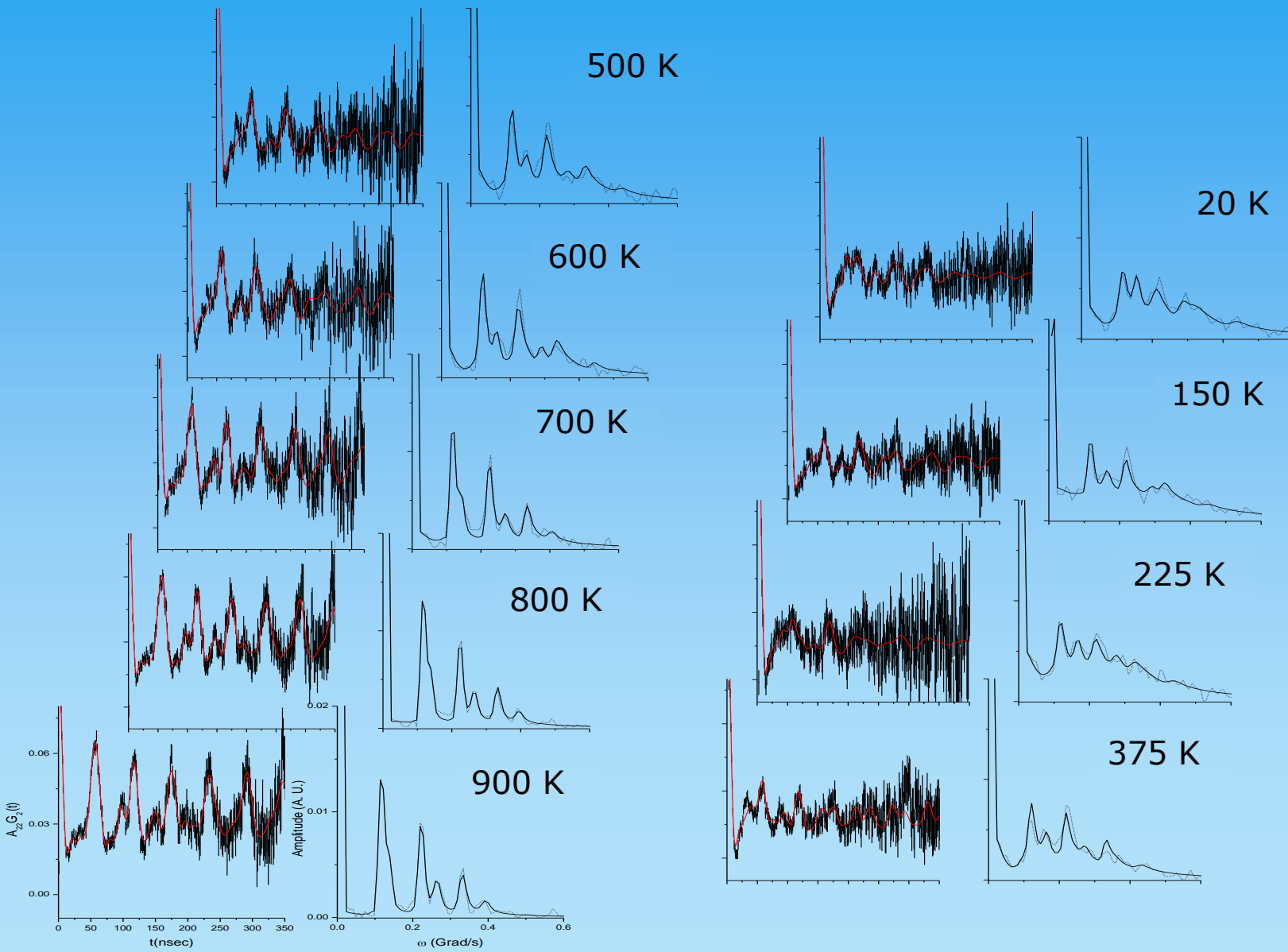
Cd- doped In₂O₃



$\text{In}_2\text{O}_3:\text{Cd}$ - HFIs vs. T



Cd-doped SnO



Charge state	Aprox.	$d_{NN} (\text{\AA})$	h	$V_{33} (10^{21} \text{V/m}^2)$
Descargada	LDA	2.257	0.000	+7.79
Neutra	LDA	2.266	0.000	+5.26
Cargada	LDA	2.368	0.000	-4.52

HFI2
HFI1

